Citrus black spot detection using hyperspectral image analysis

Duke M. Bulanon[1,2*], Thomas F. Burks[1], Dae G. Kim[1], Mark A. Ritenour[3]

(1. *Department of Agricultural and Biological Engineering, University of Florida, Gainesville, FL*;

2. *Department of Physics and Engineering, Northwest Nazarene University, Nampa, ID*;

3. *Indian River Research and Education Center, University of Florida, Fort Pierce, FL*)

Abstract: A recently discovered fungal disease called citrus black spot, is threatening the Florida citrus industry. The fungal disease, which causes cosmetic lesions on the rind of the fruit and can cause a tree to drop its fruit prematurely, could possibly lead to a ban on sales of fresh Florida citrus in other citrus-producing states. The objective of this research is to develop a multispectral imaging algorithm to detect citrus black spots based on hyperspectral image data. Hyperspectral images of citrus fruits (Valencias) were collected in the wavelength range of 480 nm to 950 nm. Five surface conditions were examined, citrus black spot, greasy spot, melanose, wind scar, and normal one. The first part of the image analysis determined the optimal wavelengths using correlation analysis based on the wavelength ratio (λ_1/λ_2) and wavelength difference ($\lambda_1 - \lambda_2$). Four wavelengths were identified, 493 nm, 629 nm, 713 nm, and 781 nm. In the second part, pattern recognition approaches namely linear discriminant classifier and artificial neural networks were developed using the four selected wavelengths as the input. Both pattern recognition approaches had an overall accuracy of 92%. The detection accuracy was improved to 96% by using the NDVI band ratio method of 713 nm and 781 nm. The multispectral image algorithm developed in this study haspotential to be adopted by a real-time multispectral imaging system for citrus black spot detection.

Keywords: citrus disease detection, hyperspectral imaging, multispectral imaging

1　Introduction

One of the many concerns facing Florida Citrus Growers is the recent spread of several plant diseases that threaten fruit marketability and tree health. Citrus canker (*Xanthomonascitri* subsp. *citri*) was found in urban Miami in 1995 and causes conspicuous and erumpent lesions on fruits, stems, and leaves, making fruit unmarketable in several countries (Gottwald et al., 2002). This disease was followed by the 2005 discovery of Huanglongbing (HLB) in Florida City, also called citrus greening, which causes blotchy mottling of leaves and leaf yellowing, eventually leads to tree decline and death (Gottwald et al., 2007). In addition to these, citrus

black spot (CBS) has been added to their list. CBS was discovered in Florida in March 2010 near Immokalee (Dewdneyet al., 2010). The Florida Department of Agriculture has confirmed black spot cases in several parts of the state and an incidence growth rate of almost eight fold in two seasons.

Citrus Black Spot (CBS) symptoms can vary in appearance but all result in cosmetic lesions on the fruit rind (Kotzé, 2000). The most typical lesion, known as hard spot, starts as small brick red spots with black margins that increase in size and develop necrotic tissue in their center. These lesions render the fruit unacceptable for many important fresh markets. In severe cases, CBS may cause premature fruit drop that reduces fruit yield. The primary source of CBS infection is ascospores produced on dead leaves on the ground and forcibly ejected into air currents and onto susceptible leaves and fruit. Lemons, grapefruits, limes,

mandarins, and late maturing orange varieties, such as Valencias, are susceptible to CBS.CBS must be effectively managed in the field to minimize its occurrence and further spread. In addition, fresh fruit packers and shippers must be careful not to ship any diseased fruit to regions or countries that prohibit it. Such a violation would harm future access to those markets.

Identifying and removing fruit with CBS symptoms is accomplished manually in the packinghouse and is a very labor-intensive and time consuming process. Developing technologies that can efficiently identify CBS-infected fruits would improve fruit quality inspection accuracy to better satisfy quarantine restriction requirements. This would also enhance the competitiveness and profitability of an industry threatened by destructive diseases and labor shortage problems. Imaging based technologies have been studied to detect citrus related diseases and defects such as fruit blemishes, leaf diseases (Pydipati et al., 2006), surface defects (Blasco et al., 2007), citrus canker (Qin et al., 2008), and citrus greening (Kim et al., 2009). Although CBS has been present in other countries for some time, there have been no studies on automatic CBS detection for existing packing facilities.

In recent years, hyperspectral and multispectral imaging techniques have emerged as useful tools for safety and quality inspection of food and agricultural products (Chen et al., 2002). Hyperspectral imaging allows the acquisition of spatial information across a sequence of individual band covering a broad wavelength range, resulting in a 3-D image cube with a high spectral resolution (GrahnandGeladi, 2007). Because hyperspectral imaging produces spectral information across tens or hundreds of bands, some of the information is redundant. Furthermore, the real-time application of hyperspectral imaging is challenging because of the large amount of data. However, the large amount of information collected from the hyperspectral data allows the selection of optimal wavelengths that are most useful for feature extraction while reducing the image data dimension. There are a number of methods that can be used to select these wavelengths from hyperspectral data.

Kim et al. (2002) used principal component analysis (PCA) to identify wavelengths for apple quality inspection. Lee et al. (2008) reported the use of correlation analysis to select wavelengths for a band ratio technique multispectral imaging approach. The selected wavelengths can be used to develop a multispectral imaging method (less than ten wavelengths), which could easily be adopted for real-time feature extraction application.

This paper presents the development of pattern recognition techniques applied to hyperspectral images for the detection of fruits infected with CBS, either as the sole blemish on fruit, or in the presence of other diseases and blemishes such as greasy spot, melanose, and wind scar. Since the raw hyperspectral image cube contained 92 bands, we identified four significant wavelengths to be used for the pattern recognition approach. The overall objective of this research was to develop a multispectral imaging method to detect citrus black spot. The specific objectives were:

1) To use correlation analysis to select the optimal wavelengths for citrus black spot detection,

2) To develop pattern recognition techniques using the selected wavelengths to detect citrus black spot in the presence of other conditions, and

3) To evaluate the performance of the pattern recognition algorithm.

2   Materials and methods

2.1   Citrusfruit samples

The fruit samples used in this study were Valencia oranges that were manually harvested in July 2010 from a CBS-infested commercial orange grove near Immokalee, FL. Along with the citrus black spot samples, four other peel conditions were collected that included greasy spot, melanose, wind scar, and unblemished peel. Figure 1 shows the color images of the five peel conditions.

Forty samples were collected for each peel condition, with a total of 200 orange samples collected and investigated in this study. All the oranges were washed and stored in an environmental control chamber maintained at 4℃. The fruit samples were removed from the control chamber two hours prior to image

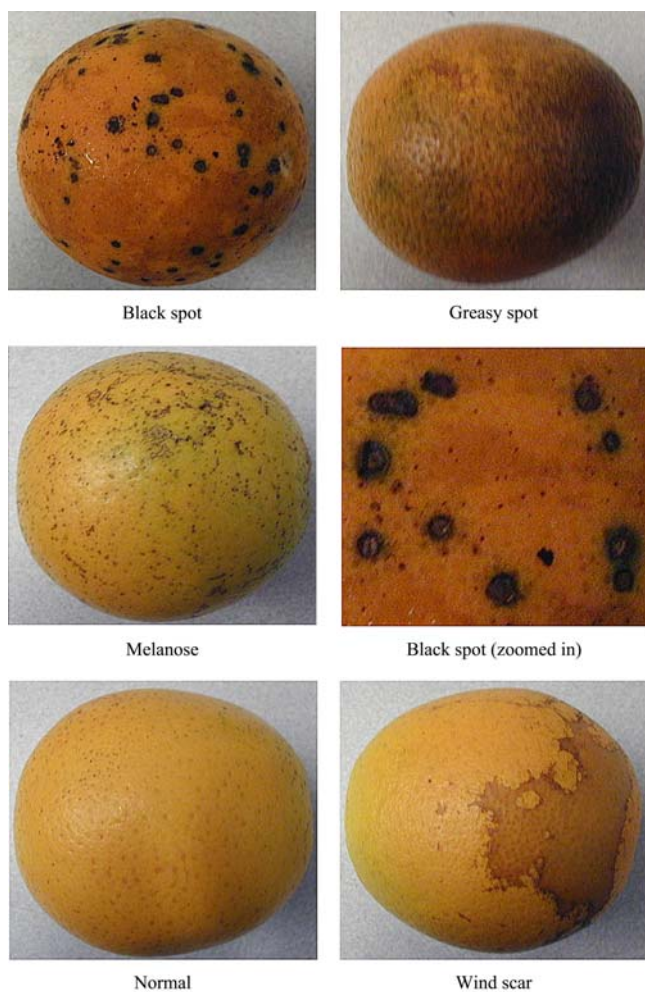acquisition to allow the fruits to reach room temperature.

Figure 1   Color images of valencia orange samples

2.2 Hyperspectralimaging system

The hyperspectral imaging system used to acquire reflectance images of the fruit samples is shown in Figure 2.   The imaging system is a push broom, line-scan type using an electron-multiplying charge-coupled device (EMCCD) camera (iXon, Andor Technology Inc., South Windsor, CT, USA).   The camera which has a resolution of 1004 × 1002 pixels is thermoelectrically cooled by a Peltier device.   An imaging spectrograph (ImSpector V10E, Spectral Imaging Ltd., Oulu, Finland) and a C-mount zoom lens were attached to the camera to acquire the hyperspectral reflectance images.   The spectrograph has a spectral resolution of 2.8 nm and an aperture slit of 30 micrometer.   This thin aperture slit limits the instantaneous field of view (IFOV) of the imaging system resulting in line scanning the samples. The reflected light from the scanned IFOV passes through the slit and is dispersed by a prism device and projected

unto the EMCCD sensor.   Thus, the resulting two-dimensional image from the EMCCD consists of the spatial dimension (line scan) and the spectral dimension (light dispersion).
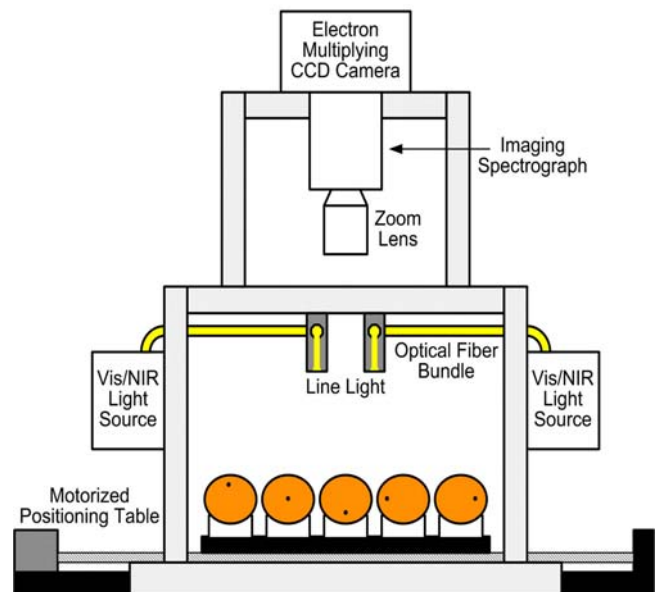

Figure 2   Hyperspectralimaging system

The lighting system comes from two line lights (21 V, 150 W halogen lights), which are arranged to illuminate the IFOV.   In this system, the camera is stationary and the sample is moved for line scanning to create a two dimensional image of the sample.   A programmable motorized positioning table (BiSLide-MN10, Velmex Inc., Bloomfield, NY, USA) is used to move the sample orange fruits.   The positioning table holds five fruits and two thousand line scans were performed to cover the five fruits.   The IFOV had 400 pixel resolution, thus generating a 3-D hyperspectral image cube with a spatial dimension of 2000 × 400 for each band.   The sample fruits were divided into 3 faces (covering 120 degree of the fruit surface), generating three scans for each fruit.

The acquired hyperspectral image has 92 spectral bands.   To correlate the each band to its specific wavelength, a spectral calibration of the system was performed using an Hg-Ne spectral calibration lamp (Oriel Instruments, Stratford, CT, USA).   To compensate for the inefficiencies of the system at wavelengths with low sensitivity of the EMCCD, only the wavelength range between 480 and 950 nm (total of 92 bands with a spectral resolution of 5.2 nm) was used in this study.   The hyperspectral imaging software control

was developed using Microsoft Visual Basic (Version 6.0) and a Software Development Kit (SDK) provided by the camera manufacturer.

2.3 Spectral data analysis

The overall hyperspectral data analysis and processing flowchart is shown in Figure 3. The hyperspectral imaging system created a hyperspectral image cube consisting of 92 bands. Prior to analysis, the relative reflectance of the hyperspectral image cube is calculated by doing a flat-field correction. Then, a correlation analysis between the peel conditions and the reflectance wavelengths is performed to obtain a multispectral image cube with only four bands. Using the reduced multispectral image data, a linear discriminant classifier and artificial neural networks were developed to detect CBS.
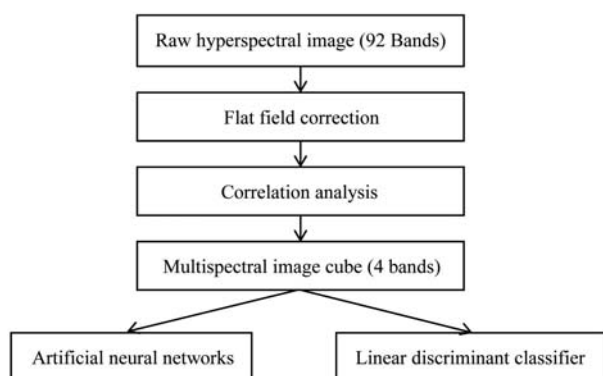

Figure 3   Hyperspectralimage analysis and processing

2.3.1   Image pre-processing

An image preprocessing procedure was performed on the acquired hyperspectral images of the orange samples prior to spectral data analysis. The preprocessing involved a flat-field correction to calculate the relative reflectance, R, of all the image scans. Equation (1) was used for the flat-field correction.

$$R = \frac{R_O(\lambda) - R_D(\lambda)}{R_W(\lambda) - R_D(\lambda)} \tag{1}$$

where, R_O is the original raw image; R_W is the image of the reflectance calibration board; R_D is the dark image which was taken by covering the camera lens with a dark cap, and λ is the wavelength. Then the relative reflectance was multiplied by 65,000 so the resulting image would be comparable to the range of the original data. An image mask was also generated by thresholding one of the images that showed a large contrast between the fruit region and the background region.

After the preprocessing operation, the reflectance spectra of the five peel conditions were collected from a specified region of interest (ROI) of the hyperspectral image data using the ENVI software (ITT Visual Information Solutions, Boulder, CO, USA). ENVI allows manual selection of the ROI using a selection tool. The ROI for each peel condition was manually selected maintaining the homogeneity of the ROI peel condition. All the orange samples were used for the ROI selections. The mean spectrum of the merged ROI for each fruit was computed and was used as the representative reflectance spectrum.

2.3.2   Wavelength selection

Correlation analysis using two wavelength combinations (band ratio and band difference) was used to determine the four significant wavelengths that could differentiate citrus black spots from the other conditions. This method is similar to Lee et al. (2008) for selecting wavelength for the detection of apple defects. Using 40 representative reflectance spectra of the five peel conditions, the two-band ratio and band difference were calculated for all possible two-band combinations. The citrus black spot condition was assigned an index value of 1, while the other four conditions were assigned an index value of 0. Correlation analysis was then performed to determine the correlation coefficients between the band combinations and the index values. The two-wavelength combination that had the highest correlation coefficient was selected as the four significant wavelengths for citrus black spot detection; λ_1, λ_2, λ_3, and λ_4. The correlation analysis was performed using MATLAB (see Equation (2) and Equation (3)).

$$Band\ ratio = \frac{\lambda_1}{\lambda_2} \tag{2}$$

$$Band\ difference = \lambda_3 - \lambda_4 \tag{3}$$

2.4 Citrus black spot detection

A multispectral image cube with the four identified wavelengths was derived from the raw data. Two pattern recognition techniques were used to classify the pixel as defect (CBS) or non-defect (CBS-free): linear

discriminant classifier (LDC) and artificial neural networks (ANN). The LDC is a linear Bayes Normal classifier which assumes normal densities with equal covariance matrices and is a function of the four wavelengths. For the ANN, a feed forward neural network classifier with four input nodes for each of the wavelength, and one output node was developed. Three configurations of the hidden layer were initially evaluated for the ANN; one hidden layer with three nodes, two hidden layer with three nodes each, and two hidden layers with four nodes each. The three configurations resulted with a similar classification error of 0.0204 after 350 numbers of epochs; therefore a configuration of one hidden layer with three nodes was selected for this study. These classifiers were developed and trained using the PRTools pattern recognition toolbox and the MATLAB neural network toolbox. The multilayer network used the log-sigmoid transfer function and was trained using the backpropagation algorithm. The training data set consisted of ten randomly picked fruits from each condition. In the multispectral image acquisition of each fruit, the fruit was divided into three faces (each face covers 120 degrees of the fruit surface), resulting in 30 multispectral images for each condition (a total of 150 training image). For each training image, a ROI of 5×5 pixels were used to extract the peel conditions.

These classifiers were then combined with the image processing algorithms to develop a CBS disease detection classification approach. A thresholding method was applied to the output image resulting from classification to segment the citrus black spots from the fruit surface background and to differentiate it from the other four peel conditions. After thresholding, a morphological filtering operation was used to remove unwanted small size pixels that could be considered as noise (Gonzalez et al., 2004). The performance of the citrus black spot segmentation was evaluated using the remaining orange fruit samples. The true positive and the false positive of the two classifiers were compared to evaluate the detection capability and obtain a method that can be adopted for a multispectral imaging solution for black spot detection in real-time. The detection accuracy is expressed by the following Equation (4).

$$Detection\ accuracy = \frac{number\ of\ fruits\ detected\ correctly}{total\ number\ of\ fruits}$$

(4)

3 Results and discussion

3.1 Hyperspectral reflectance of citrus blackspots

Representative single-band images of oranges with citrus blackspots and other peel conditions at five selected wavelengths are shown in Figure 4, to show the relative reflectance characteristics of the different peel conditions. It was observed that images less than 500 nm and greater than 900 nm appeared blurry due to the low sensitivity of the hyperspectral imaging system within these ranges. Images within the 500 nm and 900 nm showed clearly the patterns of the different peel conditions.

CBS lesions were observed at all wavelengths covered by the hyperspectral imaging system, but were more distinctive within the 500 nm to 800 nm range. Citrus black spots appear darker in the shorter wavelength but increased in intensity towards the higher wavelength range. In addition, higher contrast between the citrus blackspots and unblemished peel can be observed within the 600 nm and 700 nm range, while the contrast decreased below 500 nm and higher than 800 nm. The other peel conditions show similar characteristic with CBS, however, it was obvious that the CBS lesions had the lowest reflectance among all the peel conditions.

Figure 5 shows the typical reflectance spectra of orange samples with black spots and the other four peel conditions over the wavelength range of 480 and 950 nm. Each spectrum plot was an average of 20 spectra from 20 different samples and each of them was extracted from the hyperspectral image using an average ROI window covering 5×5 pixels. As observed with the characteristics of the hyperspectral images, the reflectance spectra showed similar patterns regardless of the peel conditions. All the conditions featured local minima at around 675 nm due to the chlorophyll presence in the fruit skin which absorbs light at this wavelength, although chlorophyll absorption for the citrus blackspots is not as distinct as the other conditions, which could be attributed to the fungal infection.
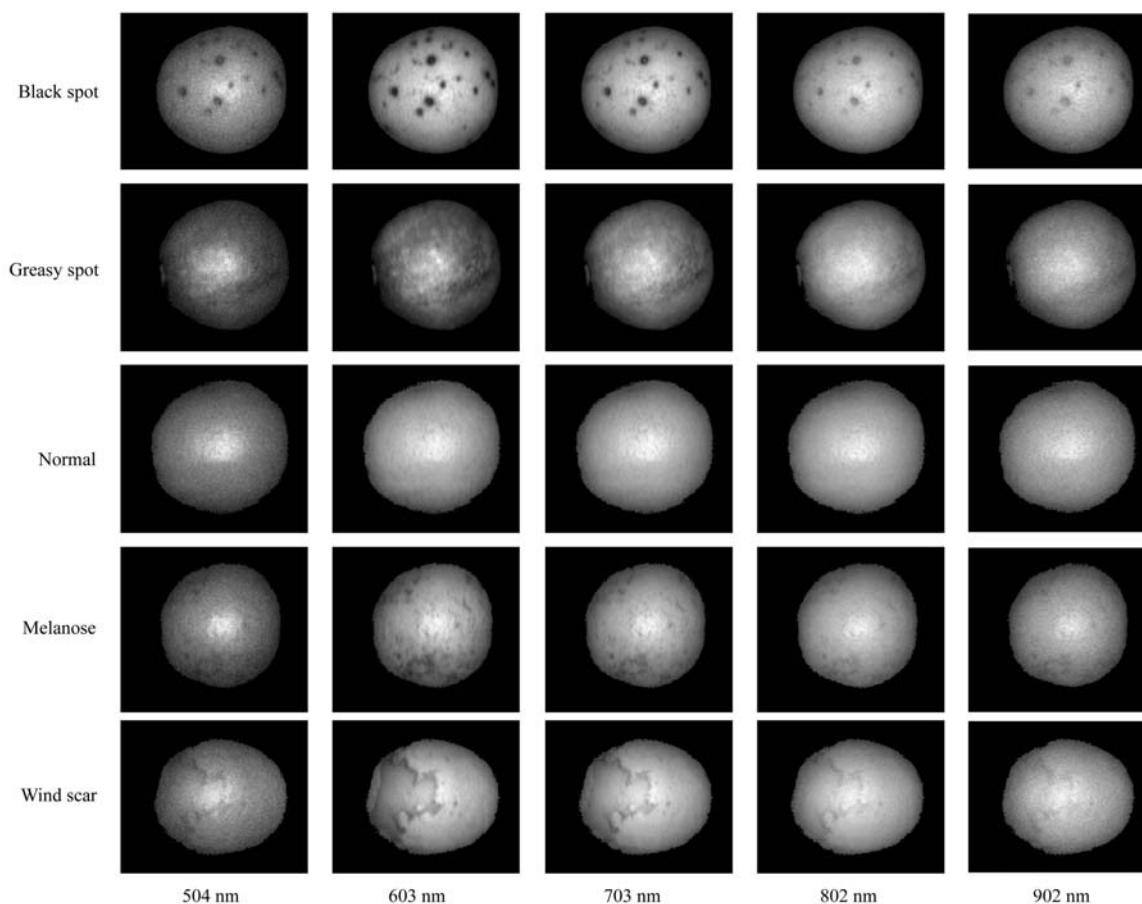
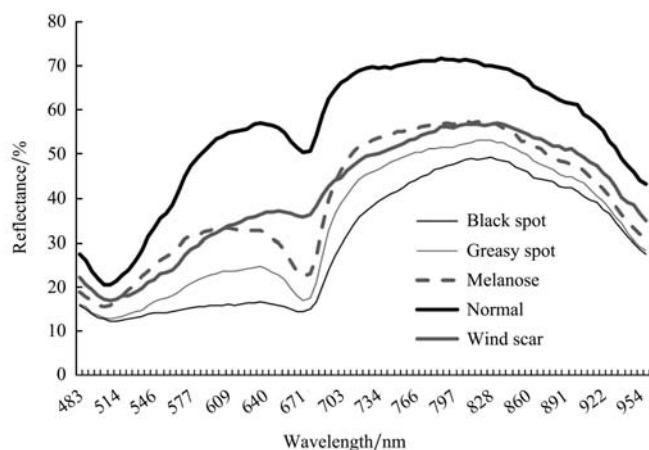Figure 4   Representative hyperspectral images of orange samples

Figure 5   Reflectance spectra of citrus black spot and other
conditions

The normal peel surface has the highest reflectance, while CBS had the lowest reflectance. This was also observed in the hyperspectral images where CBS appeared to be darker as compared with the other peel conditions. The difference of reflectance between CBS and the other conditions is very evident within the 530 nm to 650 nm range (visible range) and within the 710 nm to 800 nm range (visible near-infrared range (VNIR)). Within the visible range, the blackspots appear to be darker and it increased its intensity in the VNIR range, which was also observed with the other conditions. Although one could conclude that a conventional RGB camera can be used for detecting CBS, it should be noted that these color cameras use a wide band filter versus the narrow band filter found in hyperspectral/multispectral cameras.

3.2   Band selection

Figure 6 shows the contour plots of the correlation coefficients for the two band ratio and band difference. The two band ratio shows two regions with high correlation coefficients. One of these regions is within the visible range, where the highest correlation coefficient was found. The highest correlation corresponded to 493 nm, which is the blue band, and 629 nm, which is the green band and could be associated with chlorophyll content. The second highest correlation was observed in the VNIR region.
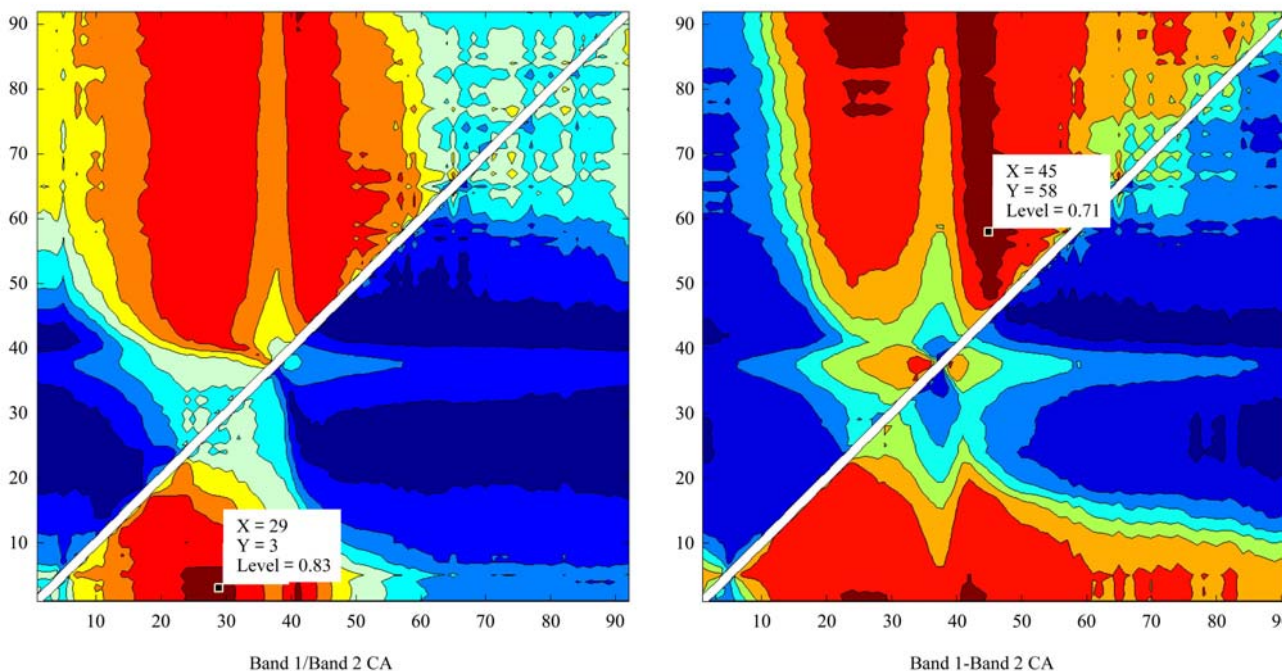
Figure 6   Contour plots of correlation analysis for two band ratio and two band difference

While the band ratio shows a high correlation within the visible range, the two band difference has the highest correlation coefficient in the VNIR region. The band difference of 713 nm and 781 nm combined for a correlation coefficient of $r = 0.80$. It was also observed that there was a region within the visible range that has a high correlation coefficient that corresponds to the area identified in the band ratio contour plot. From the two contour plots, four wavelengths were identified, two from the visible range (493 nm, 629 nm) and two from the VNIR range (713 nm, 781 nm).

3.3 Detection of citrus blackspots

Figure 7 shows the result of detecting citrus black spot using LDC and ANN on the multispectral cube of 493 nm, 629 nm, 713 nm, and 781 nm. The binary images of the citrus black spot show that both pattern recognition approaches detected the lesions correctly. There were no pixels classified as defect on the normal, melanose and wind scared ones. However, there were pixels classified as black spot lesions on the greasy spot by both approaches. This is specifically noticeable on greasy spot samples with severe infections. This could be attributed to the greasy spot reflectance characteristic which has the second lowest spectral reflectance following CBS. Table 1 shows the evaluation of LDC and ANN in detecting CBS in the presence of other peel

conditions. The two pattern recognition approaches have 100% accuracy in detecting CBS and market conditions, however, both approaches have lower detection accuracy in the presence of greasy spot with accuracies dropping to 76.7% and 73.3% for LDC and ANN respectively. The overall accuracy of both approaches is 92%. As mentioned, the similarity of the spectral characteristic of greasy spot to black spot and the severity of the condition affected the detection performance.

Table 1 Detection accuracies of LDC and ANN

	Number of Fruits	LDC		ANN	
		Misclassified	Accuracy	Misclassified	Accuracy
Citrus Black Spot	30	0	100.0%	0	100.0%
Market	30	0	100.0%	0	100.0%
Melanose	30	4	86.7%	4	86.7%
Windscar	30	1	96.7%	0	100.0%
Greasyspot	30	7	76.7%	8	73.3%
Overall			92.0%		92.0%

On the other hand, it was observed that at the VNIR range that CBS has a steeper slope as compared with greasy spot. By combining the two wavelengths in the VNIR range (713 nm and 781 nm) using Normalized Difference Vegetation Index (NDVI), it enhanced the CBS pixels. The Normalized Difference Vegetation

Index (NDVI) is a numerical indicator which can be used to analyze remotely sensed crops and is calculated from the spectral reflectance in the visible (red region) and NIR.   Since R713 is near the visible region and R781 is within the NIR, NDVI images were created from both bands using Equation (5).

$$NDVI = \frac{R781 - R713}{R781 + R713} \qquad (5)$$

Figure 8 shows how citrus black spot and its background are enhanced using NDVI.   Figures 8a and 8b are the negative images of R713 and R781.   Negative images were generated to allow relative comparison between the original images and the NDVI image.   The intensity plot of line 52, which passes through a single CBS, shows that the NDVI increased the contrast between the CBS and its background.
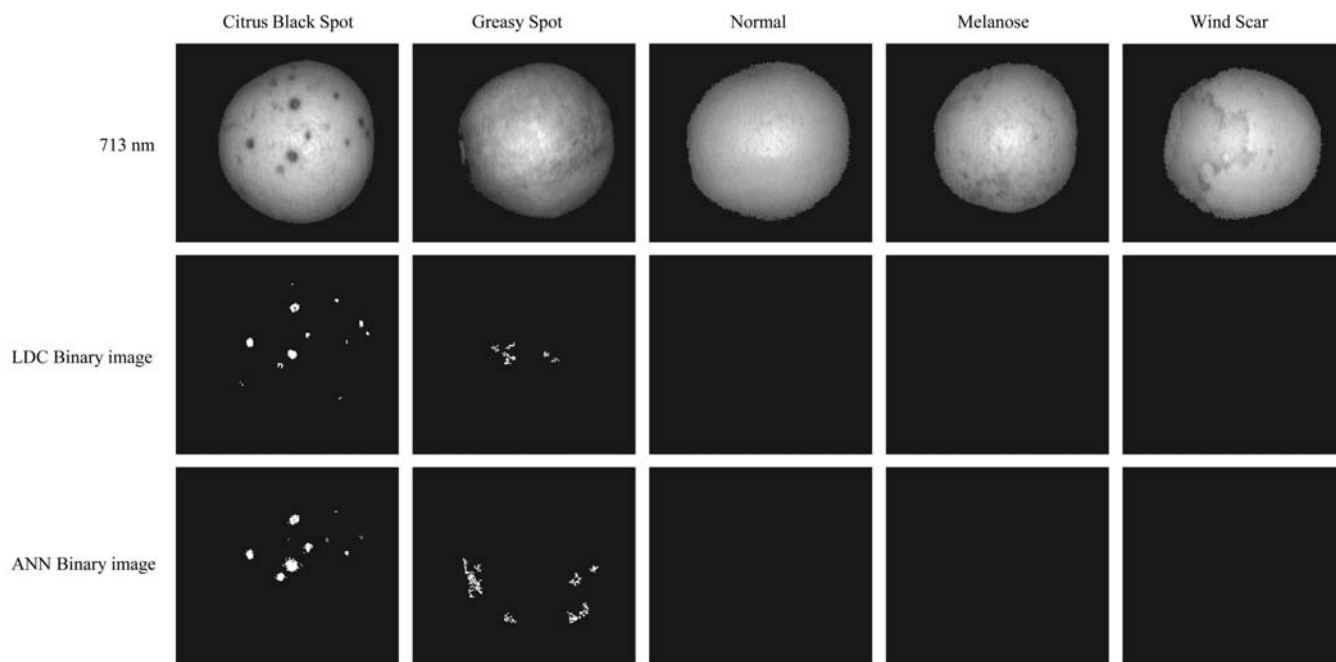

Figure 7   Detection of Citrus Black Spot Using LDC and ANN

a. Negative image of R713 image

b. Negative image of R781 image

c. NDVI image of R713 and R781
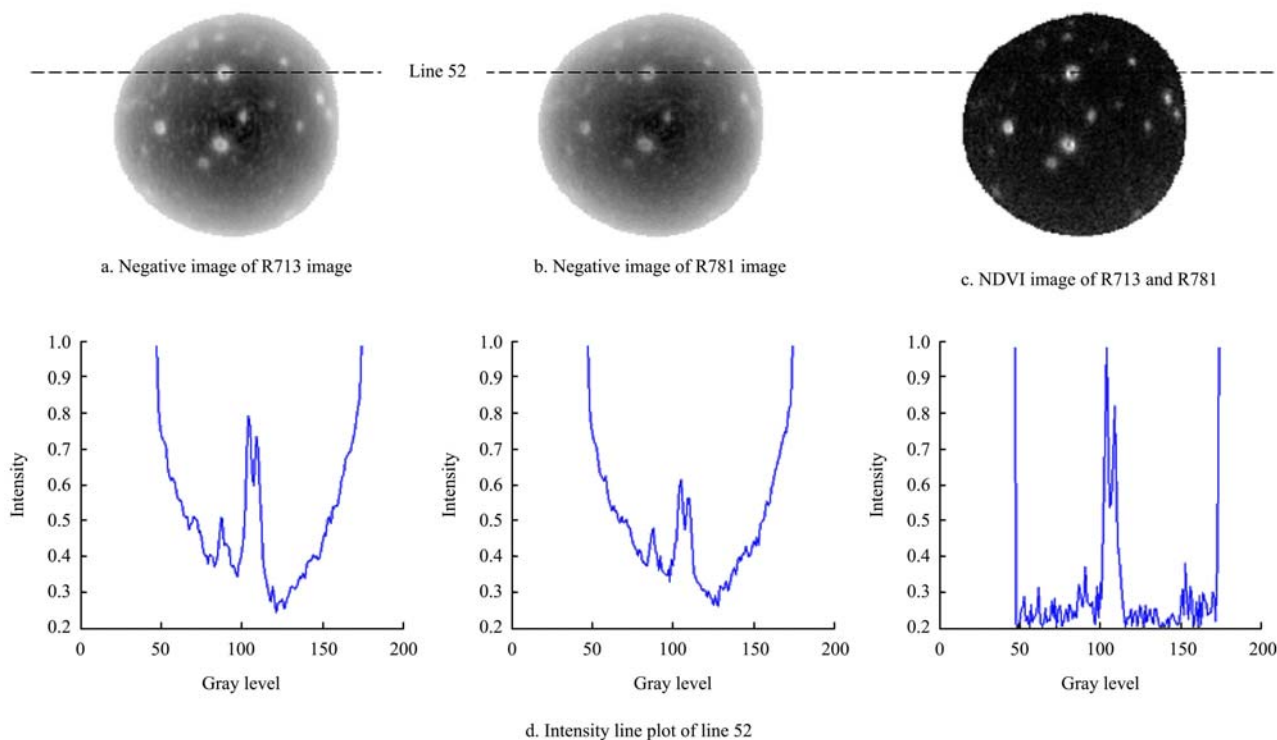
d. Intensity line plot of line 52

Figure 8   Enhancement of citrus black spot using NDVI

By using the NDVI ratio, the citrus black spot regions were intensified. The NDVI ratio method improved the detection of citrus black spot from 92.0% to 96.7% (Table 2). The ratio between the difference and the sum of the visible and NIR bands of NDVI enhanced the blackspot regions, which had a distinct spectral reflectance slope in the SNIR region, and this improved the detection accuracy. Based on these results, the selected wavelengths specifically the visible and NIR bands have the potential to be adopted by a multispectral imaging solution for real-time citrus black spot detection.

Table 2   Detection accuracies of NDVI Band Ratio

	Number of Fruits	NDVI	
		Misclassified	Accuracy
Citrus Black Spot	30	0	100.0%
Market	30	0	100.0%
Melanose	30	0	100.0%
Windscar	30	1	96.7%
Greasyspot	30	4	86.7%
Overall			96.7%

4   Conclusions

The Florida fresh market citrus industry is affected by citrus black spot, which causes cosmetic lesions on the fruit, premature fruit drop, and could disqualify the fruit for shipment to important markets. This paper presents the development of a multispectral imaging algorithm for the detection of citrus black spots in the presence of other conditions including unblemished peel, greasy spot, melanose, and wind scar. The algorithm, which is based on selecting significant bands, was derived from collected hyperspectral images of Valencia orange fruit samples that exhibited the five conditions. Correlation analyses of two band ratio and band difference were used to identify four key wavelengths that could discriminate citrus black spots. The four wavelengths identified were 493 nm, 629 nm, 713, nm, and 781 nm. Based on the results, we could conclude:

1) Both linear discriminant classifier and artificial neural networks are capable of detecting citrus black spots (100 % success rate), however false positives were relatively high in the presence of greasy spot conditions. The similarity of spectral reflectance of greasy spot to citrus black spot and the severity of the infection are the two factors that cause the false positives.

2) The NDVI of the VNIR bands improved the detection accuracy of citrus black spot from 92.0% to 96.7%. This is attributed to the steeper slope between the two bands. And because NDVI is a ratio between the difference and sum of the two bands, it enhanced the citrus black spots in the two-band image.

3) The multispectral image algorithm developed in this study has potential to be adopted as a multispectral imaging system for real-time citrus black spot detection.

References

Blasco, J., N. Aleixos, J. Gomez, and E. Molto. 2007. Citrus sorting by identification of the most common defects using multispectral computer vision. *Journal of Food Engineering*, 83(3): 384-393.

Chen, Y., K. Chao, and M. Kim. 2002. Machine vision technology for agricultural applications. *Computers and Electronics in Agriculture*, 36(2002): 173-191

Gonzalez, R. C., R. E.Woods, and S. L. Eddins. 2004. *Digital image processing using Matlab*, Pearson Prentice Hall, Upper Saddle River, New Jersey

Dewdney, M. M., N. A. Peres, M. Ritenour, T. Schubert, R. Atwood, G. England, S. H. Futch, T. Gaver, T. Hurner, C. Oswalt, and M. A. Zekri. 2010. Citrus black spot in Florida. *Citrus Industry,* 91(7): 18-21.

Gottwald, T. R., J. V. da Graça, and R. B. Bassanezi. 2007. Citrus Huanglongbing: the pathogen and its impact.Online.Plant Health Prog. http://www.plantmanage mentnetwork.org/sub/php/review/2007/huanglongbing/.(Access ed April 2011)

Gottwald, T. R., J. H. Graham, and T. S. Schubert. 2002. Citrus canker: the pathogen and its impact. Plant Health Prog.www.plantmanagementnetwork.org/pub/php/review/citrus canker/. (Accessed April, 2011)

Grahn, H. F., and P. Geladi. 2007. *Techniques and Applications of Hyperspectralimage Analysis.* John Wiley & Sons Ltd, West Sussex, England.

Kim, D. G., T. F. Burks, A. W. Schumann, M. Zekri, X. Zhao, and J. Qin. 2009. Detection of citrus greening using

Microscopic imaging. *Agricultural Engineering Internatio*nal*: the CIGR Ejournal*,Vol. XI: Manucript 1194.

Kim, M. S., A. M. Lefcourt, K. Chao, R. Chen, I. Kim, and D. E. Chan. 2002. Multispectral detection of fecal contamination on apples based on hyperspectral imagery Part 1 Application of visible and near-infrared reflectance imaging. *Transactions of the ASAE,* 45(6): 2027-2037.

Kotzé, J. M. 2000. Black spot. In *Compendium of citrus diseases*, eds.L. W. Timmer, S. M. Garnsey, and J. H. Graham, 23-25, St Paul: Academic Press Society.

Lee, K., S. Kang, S. R Delwiche, M. S. Kim, and S. Noh. 2008. Correlation analysis of hyperspectral imagery for multispectral wavelength selection for detection of defects on apples. *Sensing and Instrumentation for Food Quality and Safety,* 2: 90-96.

Pydipati, R., T. F.Burks, and W. S. Lee. 2006. Identification of citrus disease using color texture features and discriminant analysis. *Computers and Electronics in Agriculture*, 52 (1-2): 49-59.

Qin, J., T. F. Burks, M. S. Kim, K. Chao, and M. A.Ritenour. 2008. Citrus canker detection using hyperspectral reflectance imaging and PCA-based image classification method. *Sensing and Instrumentation for Food Quality and Safety*, 2(3): 168-177.